Resolution and contrast enhancement in coherent anti-Stokes Raman-scattering microscopy

Alicja Gasecka,[1,2] Amy Daradich,[1,2] Harold Dehez,[1,2] Michel Piché,[2] and Daniel Côté[1,2,*]

[1]*Institut universitaire en santé mentale de Québec, 2601 chemin de la Canardière, Québec G1J2G3, Canada*

[2]*Centre doptique, photonique et laser, Université Laval, 2375 rue de la Terrasse, Québec G1V0A6, Canada*

**Corresponding author: Daniel.Cote@crulrg.ulaval.ca*

Received August 22, 2013; revised October 4, 2013; accepted October 4, 2013;
posted October 7, 2013 (Doc. ID 195955); published October 31, 2013

We implement switching laser mode coherent anti-Stokes Raman-scattering (SLAM-CARS) microscopy to enhance the spatial resolution and contrast in label-free vibrational microscopy. The method, based on the intensity difference between two images obtained with Gaussian and doughnut-shaped modes, does not depend on the specimen and relies on minimal modifications of the typical CARS setup. We demonstrate subdiffraction resolution imaging of myelin sheaths in a mouse brainstem. A lateral resolution of $0.36\lambda_p$ is achieved.

OCIS codes: (110.0180) Microscopy; (180.5655) Raman microscopy; (190.4380) Nonlinear optics, four-wave mixing; (170.0110) Imaging systems.

http://dx.doi.org/10.1364/OL.38.004510

Optical microscopy, which is capable of nondestructive real-time imaging with molecular contrast, is an essential tool in biology. In particular, coherent anti-Stokes Raman-scattering (CARS) microscopy has been extensively used with great success to image lipid-rich structures in a broad range of tissue samples (e.g., spinal cord [1], mammary tumor [2], and mouse skin [3]). While there is a continued interest to observe tissue structure on a finer scale, optical microscopy is fundamentally limited by diffractive effects in its spatial resolution. The closest resolvable distance between adjacent scatterers ranges from 250 nm for classical optical microscopy to 400 nm for CARS microscopy [4]. Major progress has been made in this regard in fluorescence microscopy with resolution-enhancing techniques such as photoactivated localization microscopy (PALM) [5], stochastic optical reconstruction microscopy (STORM) [6], and stimulated emission depletion (STED) microscopy [7,8]. Optical-resolution enhancement in these techniques rely on manipulating the excited-state population by photochemical switching or by selective depletion of fluorophores. Unlike fluorescence, CARS is a parametric process based on coherent light-mediated coupling between the ground state and the excited vibrational state, whereby no energy is transferred from the excitation field to the molecule. The absence of an excited-state population in CARS renders the tools used to manipulate the emissive properties of molecules in fluorescence, which is not applicable to CARS microscopy.

An alternative approach for enhancing optical resolution in confocal and two-photon fluorescence microscopy has recently been proposed by two independent groups. This method, referred to as switching laser mode (SLAM) [9] or fluorescence emission difference (FED) [10] microscopy, is based on the intensity difference between two images acquired using either a fundamental Gaussian laser mode or a doughnut-shaped mode. This technique reconciles major goals of resolution enhancement for biomedical imaging: high laser powers are not required, no constraints on the specimen are present, and it is also straightforward to implement in an optical system.

In this Letter, we demonstrate that SLAM can be successfully integrated into a typical CARS microscopy setup, with minimal modifications to the setup and alignment. We first validate this technique on a well-studied model system (i.e., polystyrene beads). We then extend our study to image biological tissue; namely, myelin sheaths in a mouse brainstem. As a result, we obtain resolution and contrast-enhanced images in dense and morphometrically complex media. In conventional CARS microscopy, the sample is scanned with Gaussian beams. In order to perform the SLAM-CARS analysis, we introduce a vortex phase plate in the optical path of the pump beam [Fig. 1(a)]. Briefly, an 80 MHz, 7 ps mode-locked laser (Nd:YVO4, High-Q Laser, Austria) delivers the Stokes pulse at 1064 nm, and its second harmonic synchronously pumps an optical parametric oscillator (OPO) (Levante Emerald, APE), which generates a pump beam with approximately 400 mW of power. The OPO is tuned to 816 nm in order to probe the CH_2 symmetric stretch vibration of lipids (2845 cm^{-1}) and to 803 nm to probe polystyrene beads. The optical path of the OPO pump beam is split in two using a polarizing cube beam splitter (Thorlabs). A vortex phase plate (VVP-1a, RPC Photonics) is placed in one of the two resulting optical paths to impart a linearly varying radial phase shift to the wavefront, creating an optical vortex or doughnut mode. The two optical paths are then recombined using a second polarizing cube beam splitter (Thorlabs). By rotating the polarization incident on the first beam splitter, we can then switch between linearly polarized Gaussian and doughnut-shaped pump beams. Both Stokes and pump beams are circularly polarized using quarter-wave plates before being spatially recombined with a dichroic filter and injected into a commercial beam-scanning microscope (IX71/FV300, Olympus). For imaging, a high-numerical aperture water-immersion objective (60×, 1.2NA, UIS-UPLAPO, Olympus) was used. The backscattered anti-Stokes signal (662 nm) is collected in the epi-direction by a red-sensitive photomultiplier tube (Hamamatsu, R3896).

Two separate CARS image datasets are produced by scanning the sample using a Gaussian Stokes beam

and either a Gaussian or doughnut-mode pump beam. The image acquired using a Gaussian pump beam (as in conventional CARS microscopy) is denoted by I_g [Fig. 1(b)], whereas the image obtained using the doughnut-shaped pump beam is denoted by I_d [Fig. 1(c)]. A higher-resolution image is obtained by subtracting the two images [Fig. 1(d)]. The doughnut-shaped pattern of the imaged 150 nm bead seen in Fig. 1(c) is the result of the multiplicative interaction of the Gaussian Stokes field and the phase-shaped doughnut pump field. As the intensity distribution of the pump field decreases at its center, the object is also represented by a local minimum of intensity in the resulting image I_d. In effect, the resolution after subtraction is no longer given by the FWHM of a point-source object in I_g as in diffraction-limited microscopy, but rather by the FWHM of the doughnut-shaped ring in I_d. By virtue of the point-spread function (PSF) of the doughnut beam being larger than that of the Gaussian beam, subtraction of the two resulting CARS images will create negative values around the object. Since an object is always represented by maximum intensity in I_g and local minimum of intensity in the corresponding I_d image, negative values fall outside of the object and may be set to zero. In this method, a contrast-enhancement factor r has been introduced in the subtraction procedure $I_{\mathrm{SLAM}} = I_g - r \cdot I_d$. This factor is sample dependent: when high- and low-intensity objects are adjacent in an image, a large value for r could result in negative values that would deteriorate the quality of information found in the resultant image [11]. As with any contrast-enhancement technique, the value of r must be carefully chosen to avoid exaggerated contrast enhancement. In our analysis, we set the r value equal to one, since the average CARS signal generated by myelinated structures in our biological samples was fairly homogeneous. Moreover, to obtain a good signal-to-noise ratio, we ensure that the maximum intensities in I_g and I_d are similar. This is accomplished experimentally by adjusting the power of the Gaussian and doughnut pump beams and numerically by further normalization of the image intensities.

To study the impact of SLAM-CARS microscopy on resolution enhancement, we imaged polystyrene beads (embedded in a 2% agarose gel) whose size was much smaller than the shortest excitation wavelength used. Since λ_p used in our experiment was 816 nm, a bead diameter of 150 nm gives a value of $\sim 0.2\lambda_p$. The linear intensity profiles for 150 nm beads imaged with both Gaussian (black line) and doughnut (blue line) shaped pump beams are shown in Fig. 1(e). An average FWHM value of 330 nm for beads imaged using a Gaussian pump beam indicates that the resolution of conventional CARS microscopy is $0.4\lambda_p$. After the CARS-SLAM subtraction analysis (green line), the FWHM is reduced to 180 nm ($0.2\lambda_p$).

The ability of the CARS imaging system to resolve radiating points in close proximity is demonstrated in Fig. 2. Assuming that the resonant contribution of the CARS signal is much greater than that of the nonresonant background, and that the signal from the bulk medium (water) is effectively rejected due to the epi-detection configuration used, we can evaluate the resolution enhancement of SLAM-CARS by convolving four point sources with experimentally obtained PSFs. The PSFs used were obtained from CARS images of 150 nm polystyrene beads imaged with either a Gaussian or doughnut pump beam as in Figs. 1(b) and 1(c). Figure 2 shows CARS intensity profiles for the four scatterers located at different separation distances. The scatterers are clearly resolvable when they are separated by a distance of 400 nm ($0.5\lambda_p$) [Fig. 2(a)]. At a separation distance of 300 nm ($0.36\lambda_p$), only the SLAM-CARS approach is able to resolve four distinct objects [Fig. 2(b)]. This simulation allows us to evaluate the spatial resolution of SLAM-CARS microscopy in terms of its ability to resolve adjacent Raman-active scatterers. From this exercise, it can be seen that a lateral resolution of $0.36\lambda_p$ can be achieved with SLAM-CARS microscopy.

In order to experimentally demonstrate SLAM-CARS resolution enhancement, we imaged polystyrene beads embedded in agarose gel (2% by weight) (Fig. 2). The 350 nm polystyrene beads are clearly resolvable with

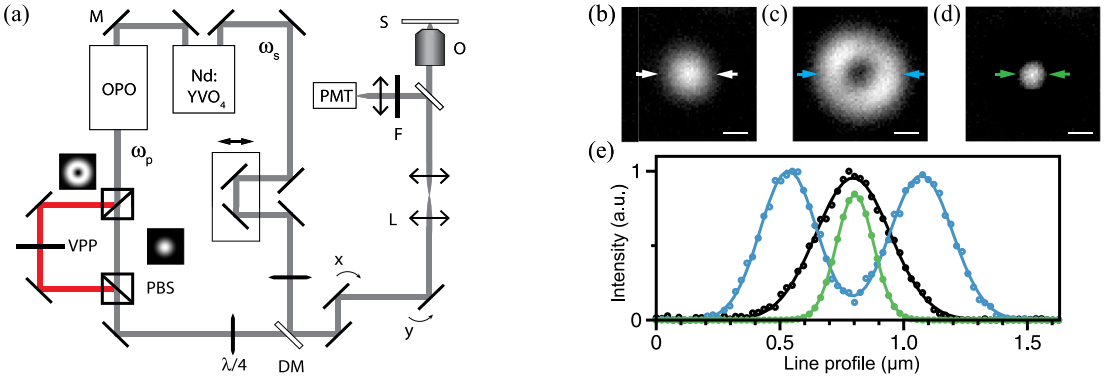

Fig. 1. (a) Conventional CARS setup (gray) and SLAM-CARS setup modification (red). The fundamental Nd:YVO_4 and OPO signal-pulse trains are used as the Stokes ω_s and pump ω_p beams, respectively. The pump beam is split in two and is either converted to a doughnut-shaped mode (red) using a VPP or is left unchanged. PBS, Polarization beam splitter; $\lambda/4$, quarter-wave plate; DM, dichroic mirror; M, mirror,; L, lens; O, objective lens; S, sample; F, anti-Stokes filter; PMT, photomultiplier tube. Experimental CARS microscopy images of 150 nm polystyrene beads embedded in 2% agarose gel for (b) Gaussian mode, (c) doughnut mode, and (d) SLAM-CARS. (e) Intensity profiles for Gaussian mode (black line), doughnut mode (blue line), and SLAM-CARS (green line). The profiles shown represent an average of the CARS signal from 10 beads. FWHM for Gaussian beam: 330 nm, FWHM for SLAM: 180 nm. Scale bars 500 nm.

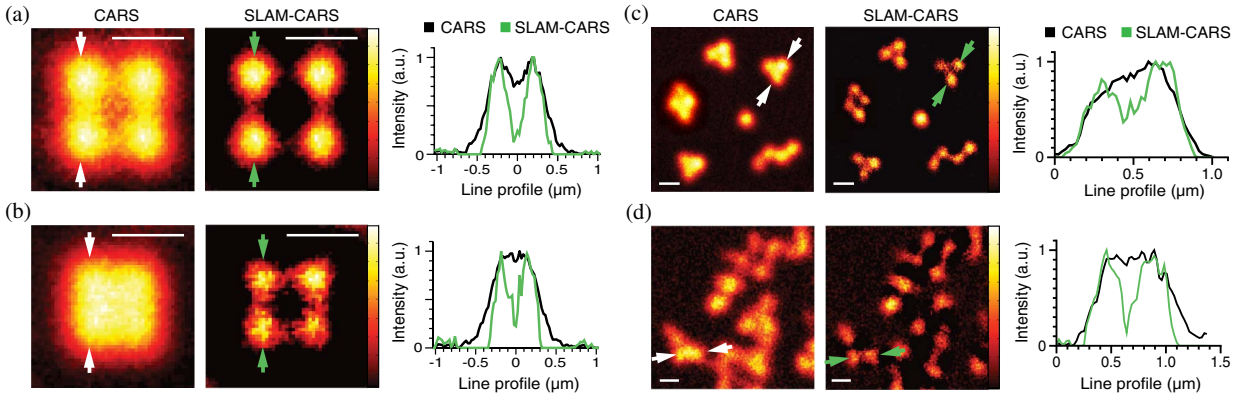

Fig. 2. Resolution and contrast enhancement realized by SLAM-CARS microscopy. CARS images of four point sources obtained by convolving experimentally obtained PSFs with adjacent radiating points separated by (a) 400 nm (the resolution limit of conventional CARS imaging) and (b) 300 nm. Plots show corresponding normalized intensity profiles evaluated along two arrowheads aligned in the vertical direction in the CARS (white arrowheads) and the SLAM-CARS image (green arrowheads). The resolution limit is defined by a 73% contrast between the peaks and the valley between the peaks. Scale bars: 500 nm. Experimental demonstration of resolution and contrast enhancement using (c) 350 nm and (d) 200 nm polystyrene beads. The images were acquired using an average pump power at the sample of 2 mW for the Gaussian pump beam, 4 mW for the doughnut-mode pump beam, and an average Stokes power of 5 mW. Images size: 4 μm × 4 μm (180 × 180 pixels). The dwell time used was 3.1 μs, and 30 frames were accumulated and averaged per image. Normalized intensity profiles are evaluated for two beads in close proximity using CARS microscopy (white arrowheads) and SLAM-CARS microscopy (green arrowheads). Scale bars 500 nm.

SLAM-CARS microscopy [Fig. 2(c)]. Within dense clusters composed of 200 nm diameter beads, the resolution enhancement is even more pronounced [Fig. 2(d)]. SLAM-CARS resolution enhancement could not be reproduced by instead using a wide variety of image-enhancement techniques in the spatial and/or frequency domain (e.g., unsharp mask, Richardson–Lucy deconvolution) on our CARS images. The unsharp mask technique does not rely on *a priori* images and can only transform the spectrum based on its amplitude. On the contrary, the SLAM-CARS technique acts by substracting two physical images, thereby affecting the amplitude and the phase of the spatial frequency spectrum of the final image. Next we demonstrate the ability of the SLAM-CARS technique to enhance resolution in morphologically complex biological tissue samples by imaging myelin sheaths in the brainstem of a mouse. Samples were obtained in accordance with guidelines from the Canadian Council on Animal Care. Mice were anesthetized and perfused intracardially with 4% paraformaldehyde (PFA) in 0.1 M phosphate buffer; the brains were postfixed overnight in the same solution at 4°C. Freshly fixed 400 μm thick slices were cut in the sagittal plane using a vibratome. Our results for CARS imaging of mouse brainstem are shown in Fig. 3. The region shown therein is largely composed of myelinated axons imaged in the transverse plane. A comparison of Figs. 3(a) and 3(b) shows that SLAM-CARS microscopy reveals the center of axons in regions that would otherwise appear continuously myelinated. This result is clearly seen in a subsection of the images (along with corresponding line profiles) shown in Figs. 3(c)–3(e). SLAM-CARS provides a technique for differentiating axons otherwise unresolved using diffraction-limited CARS microscopy as well as provides a better measure of the thickness of the myelin sheath surrounding the imaged axons. This result is of significance to morphological studies in neurology, since the size of axons relative to the thickness of myelin

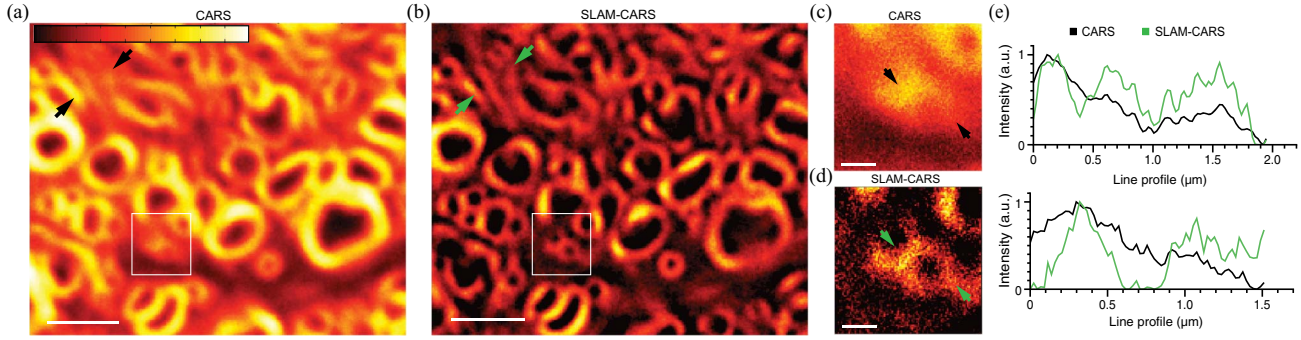

Fig. 3. Myelin sheaths in a mouse brainstem imaged with (a) standard CARS microscopy and (b) SLAM-CARS microscopy. The image was taken with an average pump power of 3 mW for Gaussian beam, 6 mW for doughnut-shaped beam, and an average Stokes power of 5 mW at the sample. Images size: 11 μm × 14 μm (500 × 600 pixels). The dwell time was 3.1 μs, and 20 frames were accumulated and averaged per image. Scale bars 2.5 μm. (c) and (d) Magnified region [CARS (c) and SALM-CARS (d)] of mouse brainstem. Scale bars 500 nm. (e) Normalized intensity profiles of the regions between arrowheads of the CARS data (black line) and SLAM-CARS data (green line) for myelin image (upper panel) and magnified region (lower panel).

surrounding them (g-ratio) is arguably one of the most important parameters considered when evaluating the pathology of demyelinating diseases.

In conclusion, SLAM-CARS microscopy allows for label-free vibrational imaging with subdiffraction-limited resolution and significant contrast enhancement. A lateral resolution of $0.36\lambda_p$. This method of imaging is a promising technique for biological applications; an optical path with a vortex phase plate is straightforward to implement and can easily be retrofitted into conventional microscopes (custom-designed or commercial units), and no limitations are placed on type of specimen used (i.e., special fluorescent markers used in other super-resolution techniques are not required) in order to achieve the resolution enhancement. Moreover, with subdiffraction-limited resolution, SLAM-CARS microscopy can be used to better map the volume, orientation, and density of myelin membranes in different regions of the brain or spinal cord, providing useful information for evaluating the pathology of demyelinating diseases. SLAM-CARS is compatible with other imaging modalities such as one- and two-photon fluorescence microscopy, reflectance imaging or sum-frequency generation. It could therefore be used in multimodal imaging platforms where the quantitative information derived from SLAM-CARS microscopy would be complementary to other techniques used.

The authors would like to thank Steve Begin and Olivier Dupont-Therrien for valuable discussions. This research was supported by the Emerging Team Program at the Canadian Institute for Health Research, the Discovery Grant program at the Natural Science and Engineering Research Council, and the Canada Research Chair program.

References

1. H. Wang, Y. Fu, P. Zickmund, R. Shi, and J. X. Cheng, Biophys. J. **89**, 581 (2005).
2. T. T. Le, C. W. Rehrer, T. B. Huff, M. B. Nichols, I. G. Camarillo, and J. X. Cheng, Mol. Imaging **6**, 205 (2007).
3. C. L. Evans, E. O. Potma, M. Puorishaag, D. Côté, C. P. Lin, and X. S. Xie, Proc. Natl. Acad. Sci. USA **102**, 16807 (2005).
4. J. X. Cheng, A. Volkmer, and X. S. Xie, J. Opt. Soc. Am. B **19**, 1363 (2002).
5. E. Betzig, G. H. Patterson, R. Sougrat, O. W. Lindwasser, S. Olenych, J. S. Bonifacino, M. W. Davidson, J. Lippincott-Schwartz, and H. F. Hess, Science **313**, 1642 (2006).
6. M. J. Rust, M. Bates, and X. Zhuang, Nat. Methods **3**, 793 (2006).
7. S. W. Hell and J. Wichmann, Opt. Lett. **19**, 780 (1994).
8. S. W. Hell, Science **316**, 1153 (2007).
9. H. Dehez, M. Piché, and Y. D. Koninck, Opt. Express **21**, 15912 (2013).
10. C. Kuang, S. Li, W. Liu, X. Hao, Z. Gu, Y. Wang, J. Ge, H. Li, and X. Liu, Sci. Rep. **3**, 1441 (2013).
11. R. Heintzmann, V. Sarafis, P. Munroe, J. Nailon, Q. S. Hanley, and T. M. Jovin, Micron **34**, 293 (2003).